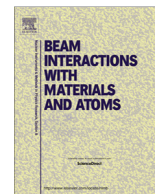




Contents lists available at ScienceDirect

Nuclear Instruments and Methods in Physics Research B

journal homepage: www.elsevier.com/locate/nimb

Role of conductivity for the production of charge patches by ions guided in capillaries

N. Stolterfoht^{a,*}, P. Herczku^b, Z. Juhász^b, S.T.S. Kovács^b, R. Rácz^b, S. Biri^b, B. Sulik^b

^a Helmholtz-Zentrum Berlin für Materialien und Energie, 14109 Berlin, Germany

^b MTA Institute for Nuclear Research (Atomki), H-4001 Debrecen, Pf. 51, Hungary

ARTICLE INFO

Article history:

Received 8 November 2016

Received in revised form 5 February 2017

Accepted 18 March 2017

Available online xxx

Keywords:

Ion transmission

Highly charged

Guiding

Nanocapillaries

Polymers

ABSTRACT

Guiding of 3-keV Ne⁷⁺ ion through nanocapillaries in highly insulating polymers was studied. By means of simulations it is made evident that oscillations of the ion emission angle after transmission through capillaries reveals charge patches within the capillaries. The creation and removal of the charge patches depend on the conductivity of the capillaries so that a relationship of the conductivity and the oscillatory structure of the mean ion emission angle can be established. Experimentally significant differences were found in the ion fractions transmitted through capillaries prepared in polycarbonate (PC) and polyethylene terephthalate (PET). For PC the ion fraction decreases with inserted charge indicating blocking effects on the transmitted ions whereas for PET the ion transmission was found to be almost constant even for long term irradiation. The observed differences were attributed to different conductivities of the capillaries in the polymer materials. This attribution was supported by additional measurements concerning the oscillatory structures of the ion emission angles.

© 2017 Elsevier B.V. All rights reserved.

1. Introduction

Since ion guiding through insulating capillaries with a diameter of hundred nanometer has been observed [1], the subject received considerable interest. Ion guiding in nanocapillaries is supported by charge patches produced by the deposition of ions within the capillary interior. The outstanding property of ion guiding is the self-organizing process, which governs the charge patch formation and the corresponding ion deflection.

Initial studies of ion guiding phenomena in insulating materials have been conducted by means of capillaries in polyethylene terephthalate (PET) [1,2]. Subsequently, several laboratories performed similar experiments using PET [3–5], polycarbonate (PC) [6,7], and other materials [8,9]. Moreover, ion guiding within single glass capillaries was observed [10–12]. Apart from the experimental work, simulations of capillary guiding [13,14] have provided additional insights into the charge patch formation. Overviews over the field studying ions and other projectiles are given in recent reviews [15,16].

In the past, particular attention has been devoted to the time evolution of the ion emission angle which revealed oscillatory structures when measured as a functions of the inserted charge

[8,17]. The oscillations can be associated with the formation of secondary charge patches temporarily created in addition to the dominant charge patch within the entrance region. It is evident that secondary charge patches can only be formed and maintained when the charge removal is limited. Thus, the charge patch formation provides information about the conductivity of the capillary material.

In general, the ion transmission rises with a time delay to a maximum where stationary (equilibrium) conditions are reached involving a constant fraction of the transmitted ions [1,2]. Only recently, experiments with PC capillaries have shown that after reaching a maximum the transmitted ion fraction decreases with charge insertion [6,7], which has been referred to as ion blocking. Additional experiments with PET capillaries [18] have shown that ion blocking increases with the areal density of the capillaries. For high densities, the neighbor capillaries create a repulsive field in a given capillary, which is responsible for the ion blocking.

Recent experimental studies, comparing PET capillaries from different laboratories, have revealed significant differences in long-term ion transmission [19]. The PET capillaries, which showed blocking [18], were prepared at the GSI Helmholtz-Zentrum in Darmstadt (Germany) [20] whereas new measurements with capillaries from the Flerov Laboratory of Nuclear Reaction (FLNR) in Dubna (Russia) [21] showed stable transmission

* Corresponding author.

E-mail address: nico@stolterfoht.com (N. Stolterfoht).

[19]. These different transmissions were associated to differences in the conductivity at the surface and bulk of the PET samples.

The present work is devoted to the comparison of transmitted ion fractions through capillaries prepared in different materials. We measured guiding of 3-keV Ne^{7+} through FLNR PET capillaries in view of the previous results obtained with the PC capillaries from GSI [6]. Significant differences were observed in the ion transmission through PET and PC capillaries, which were again attributed to different conductivities of the materials involved. This conclusion was found to be consistent with additional experiments comparing the oscillatory time dependence of the mean ion emission angle.

1.1. Trajectories and charge distributions

Before presenting the experiments, we show a few results from simulations of 4.5 Ar^{7+} ions guided through a single macrocapillary. The simulations were described in detail previously [22] so that no details about the theoretical method are given here. The capillary shape and the tilt angle were chosen in accordance with previous experiments [12]. The outstanding feature of those experiments is the control of the temperature of the macrocapillary which, in turn, allows a controlled change of its conductivity. Thus, we can demonstrate the relationship between the variation of the ion emission angle and the conductivity of the capillary material.

Such temperature variation is difficult to perform with the nanocapillaries used in the present experiments. Hence, the parameters of the calculations are not the same as those used in the present experiments. However various theoretical and experimental studies have shown that the general features of the capillary guiding through macrocapillaries and nanocapillaries are quite similar [15,16].

Fig. 1 is composed of two groups of results, which correspond to capillary bulk conductivities differing by more than an order of magnitude, i.e., 1.45×10^{-16} S/cm for the upper group and 24.6×10^{-16} S/cm for the lower group. The labels (a) to (f) refer to the increase of the ion charge Q_{in} deposited into the capillary. The left-hand and middle columns depict, respectively, ion trajectories and deposited charges within the capillary. The right-hand column shows the mean angle of the ions emitted from the capillary exit relative to the incident beam direction.

Let us first consider the upper group in Fig. 1. In panel (b) the ion trajectories are deflected by the entrance patch so that they are directly transmitted to the capillary exit. Fig. 1(c)–(f) show that the ions follow oscillatory trajectories along the capillary to the exit where they leave under varying emission angles. This can clearly be seen from the corresponding mean emission angles in the right hand column. In Fig. 1 the middle column shows the distributions of deposited charges, which allows for the distinction of the entrance patch from three additional charge patches. These charge patches are responsible for the oscillations of the ion emission angle.

Next, consider the lower group of graphs corresponding to a bulk conductivity increased by more than an order of magnitude. Fig. 1(b)–(f) shows that the ion trajectories do not change much with increasing charge insertion. The ions are deflected by the entrance charge patch directly to the capillary exit and are emitted essentially under the same angles as can be seen from the corresponding mean emission angle in the right hand column. This behavior is consistent with the middle panels, which show that no charge patches are created apart from the entrance patch. The missing charge patches are attributed to the relatively high conductivity, which rapidly depletes the deposited charges. Therefore, Fig. 1 demonstrates that the variation of the ion emission angle provides information about the conductivity of capillaries.

2. Experimental results

The experiment was carried out at the Institute of Nuclear Research of the Hungarian Academy of Sciences (ATOMKI), Debrecen. The experimental arrangement has been described in Refs. [5,19] so that only a few details shall be given here. Highly charged ions were provided by an electron cyclotron resonance (ECR) ion source [23], from which 3 keV Ne^{7+} were extracted. The beam of typically 100 pA was collimated by two diaphragms of 0.5 mm diameter spaced 20 cm apart involving a beam divergence of $\sim 0.2^\circ$ FWHM (full width at half maximum). The final charge state of the ion that passed through a capillary, could be selected using an electric deflection field in front of the ion detector.

In the experiments, capillaries in a PET sample from FLNR were used with a diameter of 200 nm and an areal densities of 1×10^8 cm $^{-2}$. These PET samples were initially prepared in Dubna by producing ion tracks by 250 MeV Kr ions and further treated at the Ionenstrahl-Labor (ISL) in Berlin by etching the ion tracks in a NaOH solution. In the previous experiments [6] with PC samples, the capillaries were prepared at GSI in Darmstadt by 2.2 GeV gold ion irradiation [20] and etching. Thus, capillaries with a diameter of ~ 165 nm and a density of 6×10^7 cm $^{-2}$ were obtained.

The capillary samples were mounted on a goniometer, which allowed for an alignment in three axial dimensions and around one rotational axis. The PET membranes were spanned on a circular frame with an inner diameter of 7 mm. In the experimental chamber the incident ions were transmitted through the capillaries and observed using a multi channel plate detector (MCP). Previous studies [2] have shown that the experimental results scale with the inserted charge so that this parameter was used to display the measured results in the following.

2.1. Total yield of the transmitted ions

The total yield Y_t for the transmission of 3-keV Ne^{7+} ions was determined by summing up the counts within an image measured by the MCP detector. The total yield was normalized by the number of incident ions Y_{in} to obtain the fraction $f_t = Y_t/Y_{in}$ of transmitted ions. In Fig. 2 the fraction f_t for the present measurements with PET capillaries is compared with previous results obtained with PC capillaries [6]. The density of the PC capillaries (6×10^7 cm $^{-2}$) is relatively high so that blocking effects due to the influence of neighbor capillaries are expected. Indeed, in Fig. 2 (a) the ion fraction exhibit an increase at the beginning of the charge insertion and after reaching a maximum the transmission curve starts to decrease by about a factor of two as Q_{in} rises from 13 to 40 fC. This decrease can be considered as the partial blocking of the ions.

In Fig. 2(b) and (c) the present results for the PET capillaries are shown. The important feature of the PET samples is that the transmission curves increase rather than decrease with increasing charge insertion, i.e., they remain stable for a charge insertion as large as $Q_{in} = 38$ fC. Hence, no blocking effects were observed for the PET capillary even for the relatively large areal density of 10^8 cm $^{-2}$. This feature for the PET capillaries differs from the corresponding results for the PC samples.

To search for an explanation, one notes that the capillary types somewhat differ in diameter, density, and tilt angle. The diameters of the PC and PET capillaries are nearly equal (165 nm and 200 nm) so that it is not expected that the capillary diameter plays an important role. However, blocking effects on PC capillaries have been found to increase with decreasing capillary tilt angle [6]. Therefore, we investigated the ion transmission through the FLNR capillaries for two different tilt angles. As seen from Fig. 2(b) and

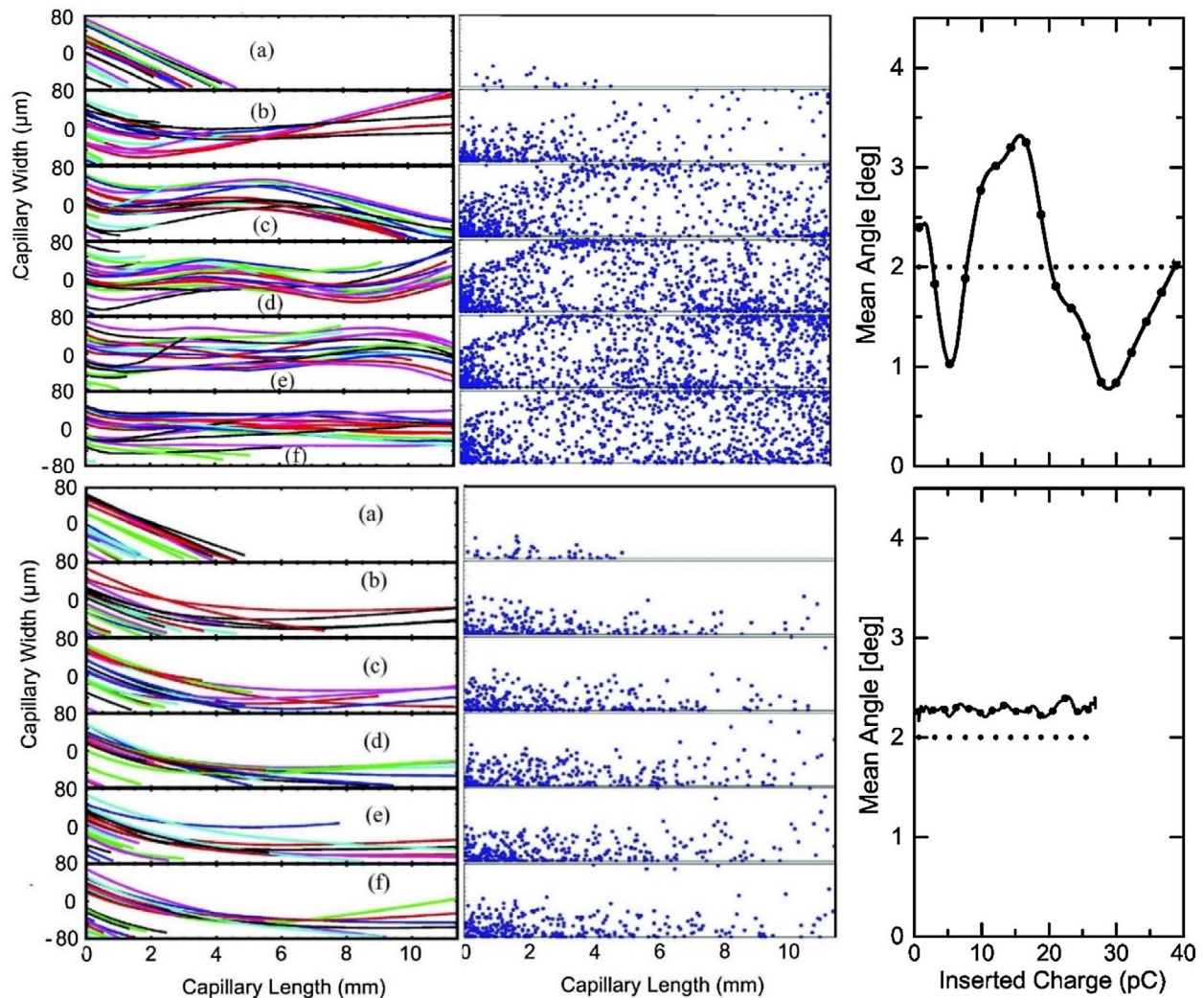


Fig. 1. Trajectories of 4.5-keV Ar^{7+} (left-hand column), distributions for the deposited charges (middle column) and mean ion emission angle (right-hand column) obtained from simulations [22]. The tilt angle is 2° . Two groups of results are shown with the capillary conductivity of 1.45×10^{-16} S/cm for the upper group and 24.6×10^{-16} S/cm for the lower group. In the upper group the inserted charge Q_{in} is equal to 0.1 pC in (a), 2.1 pC in (b), 6.8 pC in (c), 15 pC in (d), 29 pC in (e), and 58 pC in (f) and in the lower group it is equal to 0.1 pC in (a), 1.1 pC in (b), 6.8 pC in (c), 13 pC in (d), 25 pC in (e), 58 pC in (f) and 29 pC in (f).

(c) no significant difference is found between the corresponding ion transmissions.

Finally, it is noted that the density of the PET capillaries (10^8 cm^{-2}) is higher than that of the PC capillaries ($6 \times 10^7 \text{ cm}^{-2}$) for which less blocking should be expected [18] although the opposite was observed. Thus, neither the capillary density nor the capillary diameter or the tilt angle are likely to be responsible for the differences in the ion transmissions for the two sets of capillaries. Rather, in the following, we interpret the observed differences in terms of the capillary conductivities.

2.2. Emission angle of the transmitted ions

As was shown in Fig. 1, information about the capillary conductivities may be obtained from the angular emission of the transmitted ions. Thus, we measured the mean angle of ion emission from the capillary exit. In Fig. 3 results for the mean emission angle are shown for capillaries in PC and PET materials. The curves in the graphs labelled (a), (b), and (c) correspond to the cases presented in Fig. 2. All data were taken with 3-keV Ne^{7+} ions and similar tilt angles indicated in the graphs.

In Fig. 3(a) the data were measured previously using a PC sample from GSI [6]. The observed curve indicates significant oscillations, which exceeds the limits of $\pm 1^\circ$. The oscillatory structures of the mean angle reveal the formation of transient charge patches partially located within the capillary center region. Fig. 3(b) and (c) show the present results, which were measured with PET samples from FLNR. The curves exhibit a maximum at the beginning of the charge insertion whereas for higher charge values the mean angle is nearly constant.

The maximum can be associated with the formation of the entrance charge patch. Ions transmitted through the capillaries are first ejected along the capillary axis corresponding to the center angle equal to the tilt angle. Some ions, passing from the upper edge of the entrance to the lower edge of the exit, may even be ejected at angles somewhat smaller than the center angle. After the entrance charge patch has grown, the ions are reflected to angles larger than the center angle giving rise to the maximum observed for charge insertions within 2–5 fC. The subsequent constancy of mean angle allows for the conclusion that secondary charge patches are weak or missing in the inner part of the capillary. This finding provides evidence for mechanisms, which inhibit the formation of these transient charge patches.

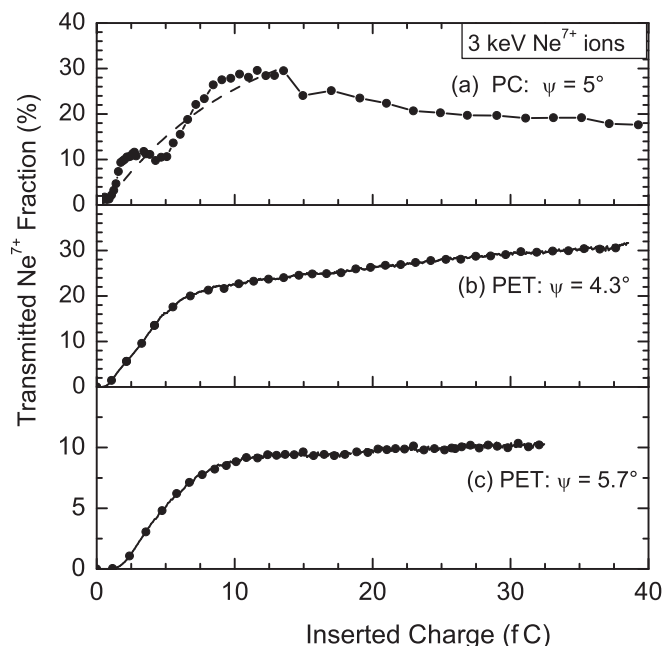


Fig. 2. Fraction f_t of 3-keV Ne^{7+} ions transmitted through polymer capillaries displayed as a function of the inserted charge Q_{in} . In (a) results for the PC sample from GSI are presented [6]. In (b) and (c) results for the FLNR PET samples are given. The tilt angles are close to 5° as indicated in each panel.

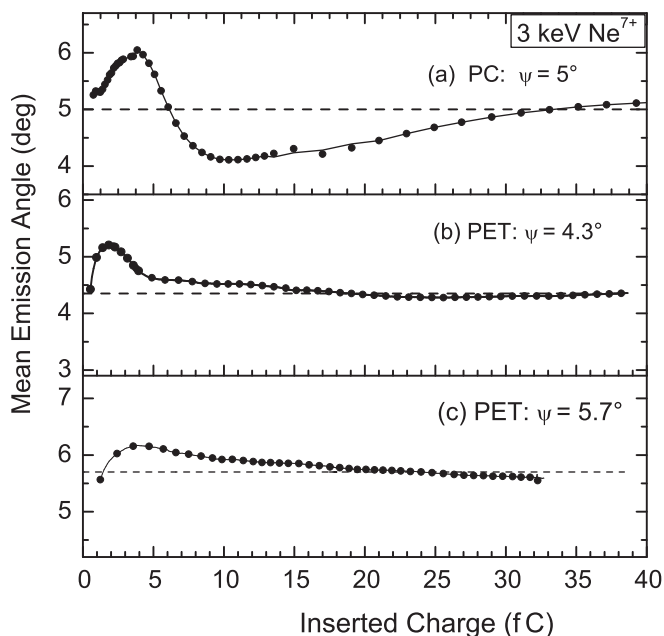


Fig. 3. Mean emission angle of 3-keV Ne^{7+} ion transmitted through polymer capillaries. In (a) results [6] for PC capillaries from GSI with a density of $6 \times 10^7 \text{ cm}^{-2}$ are displayed, in (b) and (c) results for FLNR PET capillaries with a density of $1 \times 10^8 \text{ cm}^{-2}$ are shown. The capillary tilt angles are given in each panel.

3. Discussion and conclusion

In this work, intensity and emission angle for highly charged ions transmitted through capillaries in PC and PET were studied. The capillary samples were prepared at different laboratories years ago so that it is difficult to record detailed information about the material properties. However, the experimental results can be interpreted in view of mechanisms affecting the blocking. These

effects are enhanced for capillaries of high areal density as has been found experimentally and in model calculations [18]. The ion transmission can be influenced of the charges accumulated in neighbor capillaries.

The neighbor capillaries produce a noticeable electric field along the capillary axis (z direction), which is generally small in the absence of those neighbors [14]. The induced z -field is particularly important within the capillary interior where the secondary charge patches usually occur. Oscillations of the mean angle indicate that charge patches are formed within the capillary interior and this charge is likely be responsible for the blocking effects observed for the PC sample (3(a)).

On the other hand, the missing charge patches for the PET capillaries provides evidence that the deposited charges are removed during irradiation. An efficient mechanism for charge depletion is the drift along the capillary surface to the conducting metal layers at the capillary entrance and exit [14]. With the removal of charges in the capillary neighbors, the z -field is reduced and blocking effects diminish.

Reduction of the z -field occurs for the PET sample, for which the ion transmission was found to be stable (Fig. 2(b) and (c)). Recall that the capillaries, considered here, have a relatively high areal density. Also, it should be added that in low-density PET capillaries, wherein only a small z -field is produced, no ion blocking occurs. Moreover, charge patches within those capillaries were not removed so that significant oscillations of the angular emission have been seen [18]. The latter finding supports the present scenario of charge patch formation.

Altogether, the present experiments provide evidence that in PET the capillary conductivity is higher than in PC. Data sheets for PET [24] and PC [25] indicate that their surface conductivities are similar, i.e., close to $\sim 10^{-16}$ S. However, the material properties may be affected by impurities and surface treatments, which usually imply water absorption. For PET it has been shown that the surface conductivity increases by four orders of magnitude when the relative humidity changes from 30% to 80% [24]. Moreover, the water absorption coefficient for PET is significantly larger than that for PC [24,25]. This may explain the higher conductivity evidenced for the PET samples used in this work.

In conclusion, stable transmission through capillaries is observed for materials with sufficient conductivity. The essential differences in the guiding properties for the present PET and PC samples indicate that ion blocking is not a general phenomenon for high density capillaries [19]. Hence, capillary material exists which provide long-term transmission of guided ions. This result is important for applications of ion guiding through capillaries, for which stable transmission is a mandatory condition.

Acknowledgements

This work was supported by the Hungarian National Science Foundation (OTKA, Grant No. K83886).

References

- [1] N. Stolterfoht, J.H. Bremer, V. Hoffmann, R. Hellhammer, D. Fink, A. Petrov, B. Sulik, *Phys. Rev. Lett.* **88** (2002) 133201.
- [2] N. Stolterfoht, R. Hellhammer, Z.D. Pešić, V. Hoffmann, J. Bundesmann, A. Petrov, D. Fink, B. Sulik, *Vacuum* **73** (2004) 31.
- [3] Y. Kanai, M. Hoshino, T. Kambara, T. Ikeda, R. Hellhammer, N. Stolterfoht, Y. Yamazaki, *Nucl. Instrum. Methods Phys. Res. B* **258** (2007) 1558.
- [4] M. Kreller, G. Zschornak, U. Kentsch, *Conf. Ser.* **163** (2009) 012090.
- [5] Z. Juhász, B. Sulik, R. Rácz, S. Biri, R.J. Berezcky, K. Tökési, Á. Köver, J. Pálinskás, N. Stolterfoht, *Phys. Rev. A* **82** (2010) 062903.
- [6] N. Stolterfoht, R. Hellhammer, B. Sulik, Z. Juhász, V. Bayer, C. Trautmann, E. Bodewits, R. Hoekstra, *Phys. Rev. A* **83** (2011) 062901.
- [7] Z. Juhász, S.T.S. Kovacs, P. Herczku, R. Rácz, S. Biri, I. Rajta, G.A.B. Gal, S.Z. Szilasi, J. Pálinskás, B. Sulik, *Nucl. Instrum. Methods Phys. Res. B* **279** (2012) 177.
- [8] P. Skog, H. Zhang, R. Schuch, *Phys. Rev. Lett.* **101** (2008) 223202.

- [9] H.Q. Zhang, N. Akram, P. Skog, I. Soroka, C. Trautmann, R. Schuch, *Phys. Rev. Lett.* 108 (2012) 193202.
- [10] T. Ikeda, Y. Kanai, T.M. Kojima, Y. Iwai, T. Kambara, Y. Yamazaki, M. Hoshino, T. Nebiki, T. Narusawa, *Appl. Phys. Lett.* 89 (2006) 163502.
- [11] A. Cassimi, T. Ikeda, L. Maunoury, C.L. Zhou, S. Guillous, A. Mery, H. Lebius, A. Benyagoub, C. Grygiel, H. Khemliche, P. Roncin, H. Merabet, J.A. Tanis, *Phys. Rev. A* 86 (2012) 062902.
- [12] E. Gruber, G. Kowarik, F. Ladening, J.P. Waclawek, F. Aumayr, R.J. Berezcky, K. Tökési, P. Gunacker, T. Schweigler, C. Lemell, J. Burgdörfer, *Phys. Rev. A* 86 (2012) 062901.
- [13] K. Schiessl, W. Palfinger, K. Tökési, H. Nowotny, C. Lemell, J. Burgdörfer, *Phys. Rev. A* 72 (2005) 062902.
- [14] N. Stolterfoht, *Phys. Rev. A* 87 (2013) 032901.
- [15] C. Lemell, J. Burgdörfer, F. Aumayr, *Progr. Surf. Sci.* 88 (2013) 237.
- [16] N. Stolterfoht, Y. Yamazaki, *Phys. Rep.* 629 (2016) 1.
- [17] N. Stolterfoht, R. Hellhammer, D. Fink, B. Sulik, Z. Juhász, E. Bodewits, H.M. Dang, R. Hoekstra, *Phys. Rev. A* 79 (2009) 022901.
- [18] N. Stolterfoht, R. Hellhammer, B. Sulik, Z. Juhász, V. Bayer, C. Trautmann, E. Bodewits, G. Reitsma, R. Hoekstra, *Phys. Rev. A* 88 (2013) 032902.
- [19] N. Stolterfoht, P. Herczku, Z. Juhász, S.T.S. Kovács, R. Rácz, S. Biri, B. Sulik, *Nucl. Instrum. Methods Phys. Res. B* 387 (2016) 96.
- [20] G. Pépy, P. Boeseck, A. Kuklin, E. Manceau, B. Schiedt, Z. Siwy, M. Toulemonde, C. Trautmann, *J. Appl. Cryst.* 40 (2007) s388.
- [21] Y.P. Apel, V. Ovchinnikov, *Rad. Eff. Def. Sol.* 126 (1993) 217.
- [22] N. Stolterfoht, *Phys. Rev. A* 89 (2014) 062706.
- [23] S. Biri, J. Vámosi, A. Valek, Z. Kormány, E. Takács, J. Pálkás, *Nucl. Instrum. Methods Phys. Res. B* 124 (1997) 427.
- [24] Datasheets for PET (Mylar) from DuPont Teijin FilmsTM: www.dupontteijinfilms.com.
- [25] Datasheets for PC (Lexan) from Sabic Innovative PlasticsTM: www.sabic-ip.com.